Vol. 342: 69–83, 2007 | MARINE ECOLOGY PROGRESS SERIES
Mar Ecol Prog Ser | Published July 24

Partitioning oxygen sources and sinks in a stratified, eutrophic coastal ecosystem using stable oxygen isotopes

Zoraida J. Quiñones-Rivera[1,*], Björn Wissel[1,2], Dubravko Justić[1], Brian Fry[1]

[1]Coastal Ecology Institute and Department of Oceanography and Coastal Sciences, 1209 Energy, Coast and Environment Bldg., Louisiana State University, Baton Rouge, Louisiana 70803, USA

[2]Faculty of Science and Department of Biology, 265.2 Laboratory Building, University of Regina, Regina, Saskatchewan S4S 0A2, Canada

ABSTRACT: Coastal hypoxia develops as a synergistic product of biological and physical factors. Based on oxygen concentration measurements alone, it is difficult to separate the effects of biological factors from physical factors, which complicates the analysis of oxygen dynamics. To address this problem we used a dual budget approach to assess the importance of oxygen sources and sinks for the Louisiana continental shelf in the northern Gulf of Mexico,which is strongly influenced by the Mississippi River and develops a large summertime zone of hypoxic (<2 mg O_2 l^{-1}) bottom waters. The dual budget approach was based on using stable oxygen isotopes ($\delta^{18}O$) in combination with conventional oxygen concentration measurements. The shelf ecosystem showed strong oxygen dynamics with a wide range of oxygen saturations between 180% and almost 0% and a corresponding wide range of $\delta^{18}O$ values from 15‰ in surface waters to 50‰ in bottom waters. Physical mixing primarily controlled oxygen dynamics in fall and winter, but during summer stratification, oxygen dynamics were controlled predominantly by biological processes. Model estimates indicated that during a summer 2001 shelf-wide cruise, stratified surface waters were very productive with an average calculated production/respiration (*P*/*R*) ratio of 1.12 and average gross and net primary productivities of 0.54 and 0.06 g C m^{-3} d^{-1}, respectively. In bottom waters summer oxygen depletion was predominantly due to benthic respiration, accounting for about 73% of the total oxygen loss. In the most hypoxic summer waters the importance of benthic respiration declined, consistent with low oxygen conditions slowing the rate of benthic oxygen consumption. Overall, the dual budget approach yielded new estimates of productivity dynamics in surface waters and of sediment oxygen demand in bottom waters.

KEY WORDS: Stable oxygen isotopes · Oxygen cycling · Hypoxia · Eutrophication · Mississippi River · Gulf of Mexico

INTRODUCTION

Eutrophication is often manifested in the presence of noxious algal blooms and bottom water hypoxia (<2 mg O_2 l^{-1}), which have been reported from a variety of coastal and estuarine ecosystems (Officer et al. 1984, Justić et al. 1987, Rabalais & Turner 2001). The extent and severity of eutrophication phenomena increased during the second half of the 20th century (Hickel et al. 1993, Turner & Rabalais 1994, Diaz & Rosenberg 1995), generally coinciding with increased use of fertilizer in the watersheds and higher nitrogen and phosphorus concentrations in freshwaters (Rabalais & Turner 2001). During the last 50 yr the concentration of total phosphorus and dissolved inorganic nitrogen in the Mississippi River increased 2- and 3-fold, respectively (Turner et al. 2003). In response to increased nutrient loading and eutrophication the northern Gulf of Mexico is presently the site of the largest and most severe coastal hypoxic zone in the western Atlantic

*Email: zquino1@lsu.edu

Ocean (Rabalais et al. 2002), which typically persists from April through October and extends between 5 and 60 km offshore. Abundance and diversity of demersal species are drastically reduced under hypoxic conditions (Pavella et al. 1983) and mass mortalities are known to occur among benthic infauna when bottom oxygen concentration decreases to below 0.5 mg l^{-1} (Rabalais & Turner 2001).

Hypoxia develops as a synergistic product of biological and physical factors. Nutrient-enhanced surface primary productivity results in high carbon flux to the lower water column and sediments. Decomposition of this material in bottom waters and sediments fuels oxygen consumption via bacterial respiration and decreases oxygen concentrations. Stability of the water column due to a salinity- and temperature-controlled pycnocline prevents vertical diffusive oxygen flux and prevents re-oxygenation of lower water masses by the atmosphere (Justić et al. 1996, Wiseman et al. 1997). On the other hand, wind induced mixing in fall and winter brings hypoxic waters into contact with the atmosphere and re-oxygenates the water column. This synergism of biological and physical factors complicates the development of accurate oxygen budgets. For example, a decrease in bottom oxygen content may be a result of either sediment or water column respiration. Also, an increase in oxygen content may be a consequence of *in situ* photosynthesis, oxygen influx from the atmosphere, or mixing with adjacent water masses. As a result studies based on oxygen concentration measurements alone (Justić et al. 1996) reveal only limited information about the importance of individual oxygen sources and sinks.

In recent years a second approach for measuring oxygen dynamics has been developed that uses oxygen stable isotopes ($\delta^{18}O$) in addition to conventional oxygen concentrations. Most work with oxygen isotopes has focused on open ocean systems, including the North Atlantic Ocean (Kroopnik 1975), the subarctic Pacific Ocean (Quay et al. 1993), and the subtropical Pacific Ocean (Bender & Grande 1987). Freshwater $\delta^{18}O$ studies include those conducted in the Amazon Basin (Quay et al. 1995) and the North American Great Lakes (Ostrom et al. 2005). No studies have been performed in river dominated, nutrient rich and stratified coastal waters. However, regions of intense oxygen cycling, such as the highly productive Mississippi River plume and its associated oxygen-depleted bottom waters, are expected to have highly variable $\delta^{18}O$ signals accompanying the strong fluctuations in oxygen concentrations.

Atmospheric oxygen has a $\delta^{18}O$ value of 23.5‰ (Dole et al. 1954; recent work by Barkan & Luz [2005] suggested a $\delta^{18}O$ value of 23.9‰ for atmospheric oxygen to be more accurate, but for this study we will retain a value of 23.5‰ to be consistent with the referenced literature). In a purely physical system, oxygen entering the water column from the atmosphere leads to dissolved oxygen with a $\delta^{18}O$ value of 24.2‰, due to a relatively small net equilibrium isotope effect of 0.7‰ (Knox et al. 1992, Fig. 1). Biological processes, such as photosynthesis and respiration, change $\delta^{18}O$ values from this 24.2‰ starting point. Due to the absence of fractionation in photosynthesis (Guy et al. 1993), oxygen derived from aquatic primary production has an isotope value equivalent to the oxygen of the ambient water (near 0‰ for seawater). Therefore, addition of photosynthetic oxygen in marine systems will lower the $\delta^{18}O$ of dissolved oxygen in the water from 24.2‰ towards 0‰. Water column respiration removes isotopically depleted (light) oxygen, usually with a large fractionation effect (ε) of –15 to –25‰ (Kroopnick 1975, Bender & Grande 1987, Guy et al. 1989, Quay et al. 1993, 1995, Luz et al. 2002). Hence, respiratory fractionation results in increased $\delta^{18}O$ values for the residual dissolved oxygen pool. Oxygen that is respired within the bottom sediments (hereafter referred to as benthic respiration) has a very small fractionation effect, ranging from 0 to –3‰ (Brandes & Devol 1997). Thus, a substantial contribution of benthic respiration

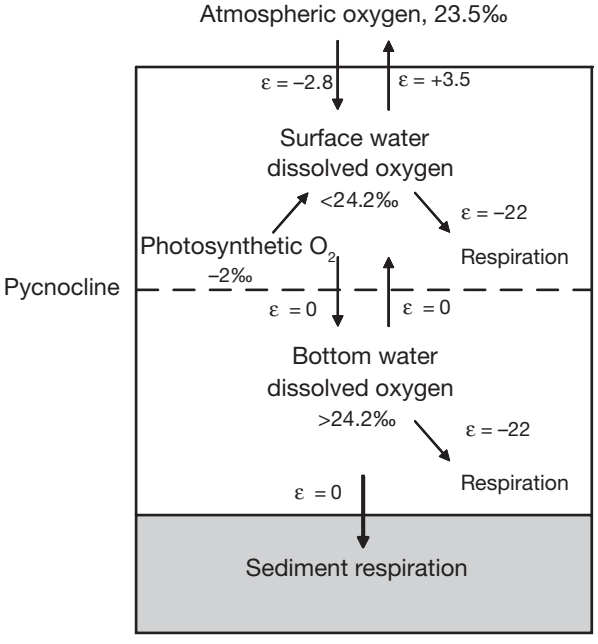

Fig. 1. Conceptual model of oxygen isotopic values for the Gulf of Mexico's hypoxic zone during stratified summer conditions. The ε symbols accompanying arrows are per mille (‰) fractionation factors (changes in $\delta^{18}O$) expected during reactions and transfers. Isotopic values are representative values taken from this study and published sources (Kroopnick 1975, Bender & Grande 1987, Guy et al. 1989, 1993, Knox et al. 1992, Quay et al. 1993, 1995, Brandes & Devol 1997)

in bottom water samples would significantly reduce the net fractionation factor.

Our objectives were to describe $\delta^{18}O$ dynamics for the hypoxic zone in the northern Gulf of Mexico and to assess the relative importance of key physical and biological processes affecting hypoxia. We investigated how the use of $\delta^{18}O$ measurements could enhance the understanding of oxygen dynamics above the level achievable with oxygen concentration measurements alone. Our study showed that the dual budget approach with both $\delta^{18}O$ and oxygen concentration measurements yielded new estimates of productivity dynamics in surface waters and of sediment oxygen demand in bottom waters.

STUDY AREA

The study area encompassed the Louisiana inner to mid-continental shelf waters in the northern Gulf of Mexico (Fig. 2). This region is strongly influenced by the Mississippi and Atchafalaya rivers, which together account for 98% of the total freshwater input into the northern Gulf of Mexico (Dinnel & Wiseman 1986). Plumes of the 2 rivers form the Louisiana Coastal Current, a highly stratified current that flows westward along the Louisiana coast and continues southward along the Texas coast. A strong seasonal pycnocline ($\Delta\sigma_t$ = 4 to 10 kg m^{-3}) persists from April to October largely due to salinity gradients. Intense wind mixing caused by frontal passages and storms can disrupt this stratification, resulting in partial or complete mixing of the water column (Wiseman et al. 1997). Primary productivity for this continental shelf region is high and averages approximately 300 g C m^{-2} yr^{-1} (Sklar & Turner 1981, Lohrenz et al. 1990). Due to the shallow water column in this region (approximately 5 to 40 m), nutrient-enhanced surface primary productivity results in high carbon flux to the sediments, and approximately 50% of the carbon produced *in situ* fuels this vertical flux (Rabalais & Turner 2001).

MATERIALS AND METHODS

Field sampling. The sampling grid consisted of 12 transects across the width of the coastal shelf from the Mississippi River Bird's Foot Delta west to the Texas–Louisiana border (Fig. 2). Each transect extended 40 to 60 km offshore and included 6 to 10 stations ranging in depth from 5 to 60 m. During a 6 d shelf-wide cruise in July 2001, surface and bottom water samples were collected at each station within each transect. In addition, from August 2001 to May 2002, surface and bottom water samples were collected during monthly monitoring cruises at each station along Transect C, 90 km west of the Mississippi River delta (Fig. 2).

During the shelf-wide cruise, Secchi depth readings (black and white disc, 25 cm diameter) were collected at stations that were sampled between 7:00 h and 19:00 h, which approximately covered the time period from 6 h before to 6 h after apparent noon.

We used a 5 l PVC Niskin sampler to collect bottom water samples and a plastic bucket for surface water. For surface samples the bucket was placed sideways onto the water surface. Once it started sinking the bucket filled passively with water avoiding intrusion of atmospheric oxygen into the sample water that could result from turbulent mixing. Surface water samples were collected approximately 10 cm below the surface while bottom water samples were collected within 1 m of the bottom sediments. Subsequently, 125 ml Wheaton glass bottles were carefully filled using plastic Tygon tubing. The tubing was either attached to the Niskin sampler (bottom samples) or water was siphoned directly from the bucket (surface samples); bottles were allowed to overflow at least twice their volume to exclude air bubbles. After filling, the bottles were immediately poisoned with 0.5 ml 6N HCl (Miyajima et al. 1995), sealed with heavy rubber stoppers (Bellco Glass, 20 mm), crimped and stored in the dark.

Isotope analyses. Immediately after their return to the laboratory samples were prepared for analysis by means of headspace equilibration (Kampbell et al.

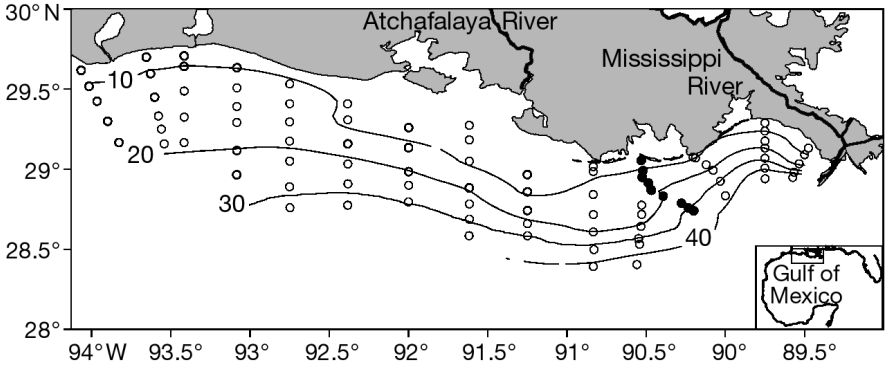

Fig. 2. Study area off the Louisiana coast in the northern Gulf of Mexico showing depth contours (m), the station grid and location of Transect C sampled each month, August 2001 to June 2002 (●)

1989, Miyajima et al. 1995). A headspace was created by injecting 10 ml of ultra-pure helium into inverted bottles while allowing 10 ml of sample water to drain out a small needle (BD brand, precision glide 23G1). The helium was injected at the bottom of the inverted sample bottle using a 15 cm long stainless steel needle attached to a 20 ml syringe (BD brand general use). Before injection the syringe was flushed 5 times with ultra-pure helium to avoid contamination with atmospheric oxygen. Subsequently, samples were stored in the dark at 5°C for 1 to 4 wk. To ensure equilibration of the dissolved gases with the headspace samples were placed in a shaker (100 rpm, room temperature) for at least 12 h before isotope analyses.

For the actual analysis a sub-sample of the headspace was injected through a septum into a helium stream. At a flow rate of 120 ml min^{-1} the sample traveled through a trap filled upstream with ascarite to absorb CO_2 and downstream with magnesium perchlorate to absorb water and a 2 m packed gas chromatography column (molecular sieve, 5 Å pore size) for separation of O_2 and N_2 for on-line,continuous flow isotope ratio measurements. To optimize signal strength the amount of headspace injected varied with the dissolved oxygen concentration in the sample, which was measured in the field using a Hydrolab instrument (Hach). Accordingly, 1, 3, or 5 ml of headspace were injected for dissolved oxygen concentrations of >7, 7–2, or <2 mg l^{-1}. Before each injection the syringe (BD brand general use, Luer-Lok tip) was flushed 5 times with ultra pure helium and subsequently pressurized (150 kPa) using a 3-way stopcock. After a new needle (BD brand, precision glide 23G1) was attached the syringe was opened to release pressure and expel any air and quickly adjusted to the desired injection volume, which was then injected into the headspace. After thoroughly mixing the ultra-pure helium with the headspace the desired amount of sample was withdrawn and immediately injected into the helium stream for analysis.

The gas analysis system allowed sequential elution of oxygen and nitrogen gases so that concentrations of both dissolved oxygen and nitrogen could be calculated using the peak areas of mass 32 and 28, measured respectively, in a downstream isotope ratio mass spectrometer (IRMS). The peak areas were calibrated using laboratory standards prepared in the same manner as samples, but air equilibrated artificial seawater was used as a water source. This artificial seawater was prepared by adding 33.75 g l^{-1} of NaCl to distilled water in a 4 l glass beaker, then stirred overnight to achieve equilibration. The stirring speed was adjusted to obtain a small vortex of <5 cm height to avoid supersaturation. After equilibration and just before filling these bottles with standard seawater we added 2000 µmol $l^{-1}$of $NaCO_3$ to match the dissolved inorganic carbon (DIC) concentration of natural seawater.

Procedural blanks were prepared in the same way as procedural artificial seawater standards, but to obtain zero-oxygen water, 50 g l^{-1} Na_2SO_3 were added (Kampbell et al. 1989). The average oxygen concentration of zero-oxygen blanks was 0.007 mg l^{-1} (±0.002 standard deviation [SD], n = 32), which corresponded to 0.1% and 0.3% of the average surface (7.0 mg l^{-1}) and bottom (2.1 mg l^{-1}) oxygen concentration during the shelf-wide cruise, respectively. Accordingly, oxygen concentrations and isotopic values for all samples were corrected by subtraction and mass balance, respectively.

The isotope values of oxygen ($\delta^{18}O$ expressed as ‰ relative to standard mean ocean water, SMOW) were determined using a Finnigan Thermoquest Delta plus IRMS. As the primary standard we used air (Dole et al. 1954) with a known $\delta^{18}O$ value of 23.5‰ (±0.17 SD, n = 89). The saturated artificial seawater used as procedural standard gave the expected $\delta^{18}O$ value of 24.2‰ (±0.21 SD for $\delta^{18}O$, n = 83) as well as accurate dissolved oxygen and nitrogen concentrations, whereby the saturation concentrations were calculated according to Weiss (1970) using known temperature and salinity.

To investigate the precision of our analyses we collected replicate samples of surface and bottom water (n = 19) during the cruise in October 2001. The average difference for oxygen concentrations and $\delta^{18}O$ values were 0.11 mg l^{-1} (±0.16 SD) and 0.05‰ (±0.04 SD), respectively.

Because headspace injections were not carried out using high precision syringes, inaccurate injection volumes (±0.1 ml) sometimes affected our oxygen concentration measurements. Depending on the injection volume (1 to 5 ml) this injection error varied between ±2 to ±10% of the ambient oxygen concentrations. The largest potential for error was related to extremely supersaturated surface water samples due to their small injection volumes (1 ml), while bottom water samples with the largest injection volume (5 ml) were the least affected. Nevertheless, because dissolved nitrogen gas is generally inactive and should be close to 100% saturation in water samples, the parallel measurement of oxygen and nitrogen concentrations from the same sample allowed us to calculate the magnitude of over- or under-estimation of nitrogen gas concentrations due to injection errors in our samples. Saturation levels for dissolved oxygen and nitrogen were calculated according to Weiss (1970) by obtaining temperature and salinity readings taken with the Hydrolab at the approximate time and depth of sampling. Subsequently, we could correct the amounts of oxygen based on N_2 saturation levels in individual samples

assuming that dissolved nitrogen was 100% saturated as follows:

$$(O_2)_{N2corrected} = 100 \times (O_2)_{measured}/N_2saturation_{measured}$$

This correction was solely a volumetric correction affecting oxygen concentrations and as such did not affect the $\delta^{18}O$ values and did not entail any $\delta^{18}O$ correction.

The assumption of nitrogen being inactive holds true for surface waters, which are generally not supersaturated by more than 2% (Benson & Parker 1961, Craig & Hayward 1987, Emerson et al. 1999). For bottom water samples intense denitrification producing N_2 could have increased the dissolved nitrogen concentrations above saturation levels. We actually observed a trend of increasing nitrogen concentrations at low levels of oxygen (Fig. 3), whereby the average N_2 super-saturation in bottom water samples was approximately 7%. Still, even a 10% N_2 supersaturation would only have a small effect on the oxygen correction, e.g. a measured oxygen concentration of 1.0 mg l^{-1} would change to 0.9 mg l^{-1}. For future studies, oxygen/argon (O_2/Ar) ratios should be used instead of O_2/N_2 as Ar gas is truly inert and would further reduce uncertainties, especially for bottom water samples.

Overall, we made this adjustment of oxygen concentrations based on nitrogen saturation levels because the correction significantly improved the data set so that the laboratory oxygen concentration estimates better matched the field Hydrolab measurements (which were routinely calibrated using Winkler dissolved oxygen measurements during all cruises). Thus, after these corrections, the r^2 value of calculated O_2 concentrations versus measured Hydrolab values for the 2001 shelf-wide cruise samples increased overall from 0.92 to 0.97, while for surface and bottom values individually, the r^2 increased from 0.66 to 0.83 and 0.80 to 0.96, respectively. The lower final r^2 values for surface samples can be explained by the smaller range of oxygen concentrations from about 6 to 8 mg l^{-1} (with the exception of 5 samples exceeding 10 mg l^{-1}), while bottom water O_2 concentrations were between 0.5 and 7.0 mg l^{-1}. As this was the first attempt to measure both oxygen isotopes and concentration from the same IRMS analysis, the Winkler-calibrated Hydrolab data were important to validate the reliability of our calculations. Even though oxygen concentrations were acquired shipboard using a Hydrolab we made the oxygen corrections to the laboratory analyses as described above and then relied on the laboratory oxygen concentration measurements for reasons of consistency.

To obtain a fractionation factor for water column respiration that was representative for our system we incubated surface water that was collected during 3 cruises along Transect C (October 2002, March and July 2003). For each incubation experiment 12 sample bottles were filled with surface water from a single bucket haul at Station C6b. While 3 samples were immediately preserved with HCl to stop biological activity (t_0), 9 bottles were closed without preservation. These 9 samples were then incubated in the dark to only allow respiration, and at each of 3 subsequent time steps (t_1, t_2, and t_3) 3 more samples were preserved. Subsequently, we calculated an average system-specific fractionation factor for water column respiration (–22.0 ± 0.7‰, Fig. 4) according to Mariotti et al. 1981.

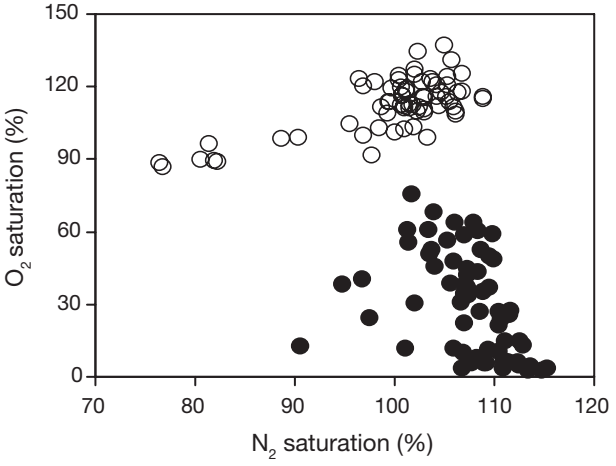

Fig. 3. Relationship between measured oxygen (O_2) and nitrogen (N_2) saturation for surface (○) and bottom samples (●) collected during the shelf-wide cruise, July 2001

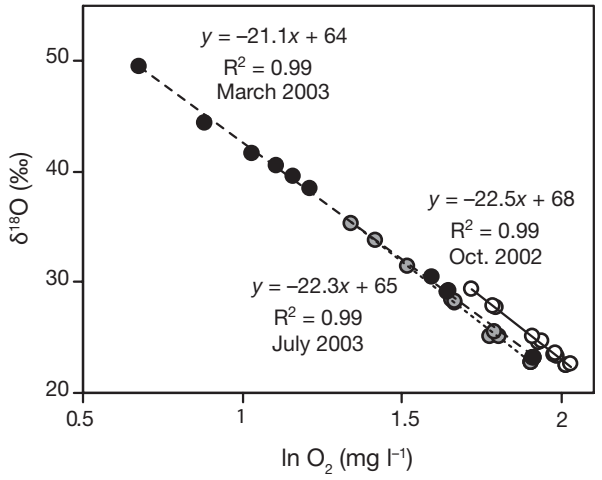

Fig. 4. Experimentally determined fractionation factors for water column respiration in surface waters on the Louisiana continental shelf. Samples were collected at Station C6b along Transect C in October 2002 (○), and in March (●) and July (◍) of 2003. Incubation times were 37, 26 and 8 d, respectively. The negative slope of the linear regression represents the fractionation factor (Mariotti et al. 1981)

Modeling approach. To evaluate oxygen dynamics recorded in the combined measurements of oxygen concentrations and $\delta^{18}O$ values we developed a finite difference model equivalent to that used by Bender & Grande (1987) with sequential steps for mixing, fractionation, and air–sea gas exchange (Fry 2006). The mixing pertains to new oxygen added from photosynthesis or gas invasion and the fractionation pertains to oxygen removed by respiration or gas evasion. Isotope mixing can be understood as a weighted average while isotopic fractionation for respiration can be described by logarithmic distillation equations (Mariotti et al. 1981). The 8 sequential equations used in each time step of the model were:

(1) Oxygen gain during photosynthesis:

$$S_{S1} = S_{INITIAL} + C_P$$

(2) Isotope mixing during photosynthesis:

$$\delta_{S1}S_{S1} = \delta_{INITIAL}S_{INITIAL} + \delta_P C_P$$

(3) Oxygen gain during invasion

$$S_{S2} = S_{S1} + C_I$$

(4) Isotope mixing during invasion:

$$\delta_{S2}S_{S2} = \delta_{S1}S_{S1} + \delta_I C_I$$

(5) Oxygen loss during respiration:

$$S_{S3} = S_{S2} - C_R$$

(6) Isotope fractionation during respiration:

$$\delta_{S3} = \delta_{S2} + \varepsilon_R \ln((S_{S2} - C_R)/S_{S3})$$

(7) Oxygen loss during evasion:

$$S_{S4} = S_{S3} - C_E$$

(8) Isotope fractionation during evasion

$$\delta_{S4} = \delta_{S3} + \varepsilon_E \ln((S_3 - C_E)/S_4)$$

where δ is the $\delta^{18}O$ value, S is percent saturation of oxygen, ε_R and ε_E are the fractionation factors (negative in sign, Mariotti et al. 1981) associated with respiration and evasion, C is the change in oxygen saturation associated with photosynthesis, respiration, or air-sea gas transfer, and subscripts are as follows: P = new oxygen added from photosynthesis, I = new oxygen added by invasion, R = oxygen removed by respiration, E = oxygen removed by evasion. In practice, these equations are linked in a row of calculations in a spreadsheet and then the last values of a row are used as initial values for the next row, i.e. S_4 and δ_{S4} from the end of one row become the initial values of the next row (Fry 2006) so that one row represents a complete cycle of photosynthesis + invasion + respiration + evasion accumulated in one time interval. To complete the parameterization of these models we selected the following values: $\delta^{18}O$ value of –2‰ for new photosynthetic oxygen (based on an average salinity of 30‰, assuming mixing of Mississippi River water with a $\delta^{18}O$ value of –7‰ [Kendall pers. comm.] with full strength salinity water of 0‰), $\delta^{18}O$ value of 24.2‰ for invading atmospheric oxygen (Knox et al. 1992), ε_R = –22‰ for respiration in surface waters (average value from 3 incubation experiments, see above), ε_R = 0‰ for respiration in sediments (Brandes & Devol 1997) and ε_E = –3.5‰ (derived from data presented in Knox et al. 1992).

Model runs typically started from initial conditions of 100% oxygen saturation and 24.2‰ $\delta^{18}O$ set by equilibration with the atmosphere. The equations were propagated over 100 to 10000 time intervals using incremental changes in concentration for photosynthesis (C_P), respiration, (C_R), and air-sea gas exchange (C_I and C_E), and resulting curves were fit to experimental data as shown in Figs. 5 & 12 (below).

We used these finite difference models to estimate production/respiration ratios (hereafter, *P*/*R*) in surface waters, and respiration dynamics in bottom waters. To estimate *P*/*R* for individual samples of surface water we started from a fixed point of air-equilibrated seawater (100% saturation, 24.2‰ $\delta^{18}O$). The respiration rate was held constant at 0.07 mg O_2 l^{-1} h^{-1}, which was the average decrease in O_2 concentration during 3 consecutive nights (photosynthetically active radiation [PAR] = 0) during the July 2001 shelf-wide cruise. The r^2 value between oxygen concentration and time for these nights was 0.54, with the first night-time period excluded from the regression due to the large inhomogeneity of surface water masses near the mouth of the Mississippi River. Air–sea gas exchange was dependent on oxygen saturation levels and wind speed (Stigebrandt 1991), which was 5.5 m s^{-1} (± 2.1 SD) during the sampling period from July 21 to 26, 2001 (measured shipboard using a RM Young 05103 Wind Monitor).

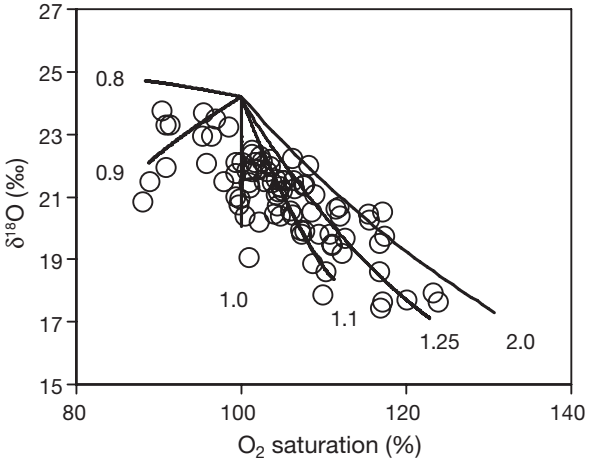

Fig. 5. Relationship between oxygen saturation and $\delta^{18}O$ for surface water samples collected during the shelf-wide cruise, July 2001. Lines represent oxygen saturation and $\delta^{18}O$ values modeled for production to respiration ratios (*P*/*R*) between 5.0 and 0.8. Data points of stations with oxygen saturation greater than 140% (n = 4) were above the *P*/*R* = 5 line and could not be modeled

We found little evidence for benthic photosynthesis or gas exchange with the upper water column for bottom waters in our sampling area (see below) and we refocused this model to estimate fractionations associated with respiration only, assuming benthic photosynthesis and gas exchange to be zero. This respiration only formulation of the model generated curves from a starting point of air-equilibrated seawater (100% saturation, 24.2‰ $\delta^{18}O$) that intersected individual data points depending on the fractionation factor used during respiration (ε_R in Eq. 6 above). Estimates of the individual ε_R fractionation factors were used to partition the sources of respiration with sediment respiration expected to occur with no fractionation and respiration in bottom waters expected to occur with a fractionation of −22‰. Thus, the estimated ε_R values were intermediate between 0‰ ($\varepsilon_{benthic}$) and −22‰ ($\varepsilon_{water\ column}$) with values closer to 0‰ indicating stronger sediment respiration, according to the formula:

$$\% \text{ benthic respiration} = 100 \times (\varepsilon_{observed} - \varepsilon_{water\ column}) / (\varepsilon_{benthic} - \varepsilon_{water\ column})$$

Nevertheless, to investigate the potential effect that benthic photosynthesis or gas exchange with the upper water column could have had on bottom water oxygen dynamics we included Eqs. 1 through 4 (photosynthesis and invasion; evasion was not included as bottom waters were always undersaturated) into the model for bottom waters. For each time step we allowed 20% of the respired oxygen to be added back into bottom waters by either benthic photosynthesis or gas exchange with the upper water column, whereby the $\delta^{18}O$ values for these 2 oxygen sources were respectively −2 and 21‰ (average $\delta^{18}O$ value of surface waters during this study). Subsequently, we re-calculated the $\delta^{18}O$ versus O_2 saturation curves for these scenarios and compared them with the original model that was based on respiration only.

All spatial diagrams were developed using Surfer Version 8.02 (Golden Software). The spatial interpolation between individual sampling points was performed using the kriging technique. In the interpolations we used standard features of the software to account for variable spacing between stations and transects.

RESULTS

Seasonal trends

Monthly sampling along Transect C (Fig. 2) showed strong seasonal variability of oxygen concentrations and $\delta^{18}O$ throughout the development and dissipation of hypoxia. Comparisons of fall and summer transects illustrate these seasonal patterns. In fall and winter, shorter days and strong winds, along with reduced river discharge and reduced nutrient loading, usually favor relatively low primary productivity and high aeration of shallow (<100 m) Gulf of Mexico waters. In October oxygen in both surface and bottom waters was at saturation and $\delta^{18}O$ values were very close to 24.2‰, the expected value for air-equilibrated seawater (Fig. 6). On the other hand when fairly calm summertime conditions prevailed in August surface phytoplankton blooms developed and produced oxygen supersaturation, while bottom waters became depleted in oxygen and saturation declined to near-zero levels (Fig. 6). Along with these intense changes in oxygen concentrations there were strong, but inverse changes in $\delta^{18}O$. Surface $\delta^{18}O$ values were below 24.2‰ when waters were supersaturated with oxygen, while in bottom waters when oxygen concentrations were low we observed high $\delta^{18}O$ values up to 50‰ (Fig. 6). Overall, we found a strong negative (or inverse) correlation between oxygen concentrations and $\delta^{18}O$ values during this seasonal study.

Beyond these obvious seasonal contrasts we observed interesting variations in oxygen concentrations and $\delta^{18}O$ on a shorter time scale when monthly sampling showed that oxygen depletion could also occur in winter (Fig. 7). During calm periods in winter oxygen saturation in surface waters often exceeded 130% and bottom water oxygen saturation could drop to 60% (Fig. 7). Accordingly, at higher oxygen concentrations in surface waters $\delta^{18}O$ values decreased to about 18‰, while at lower concentrations in bottom waters $\delta^{18}O$ values increased to 28‰ (Fig. 7). Only recurring, strong physical mixing was capable of re-oxygenating the whole water column and well-mixed conditions were observed in October 2001 and February through March 2002. Overall, the system was quite dynamic with respect to oxygen concentrations and $\delta^{18}O$ values displaying intense spatial variations in addition to month-to-month variations. For example, the location of minimum oxygen concentration (Fig. 7) moved from onshore during November and December 2001 (water depths less than 15 m) to offshore in January and February of 2002 (stations between 20 and 30 m water depth).

Surface water dynamics in July 2001

During the shelf-wide cruise in July 2001 oxygen concentrations of surface waters were always high, generally exceeding 100% saturation. The highest concentrations of 10 to 14 mg l^{-1} were observed near the mouth of the Mississippi River, while elsewhere the oxygen concentrations were between 6 and 8 mg l^{-1} (Fig. 8). Due to the continuous 24 h sampling scheme a

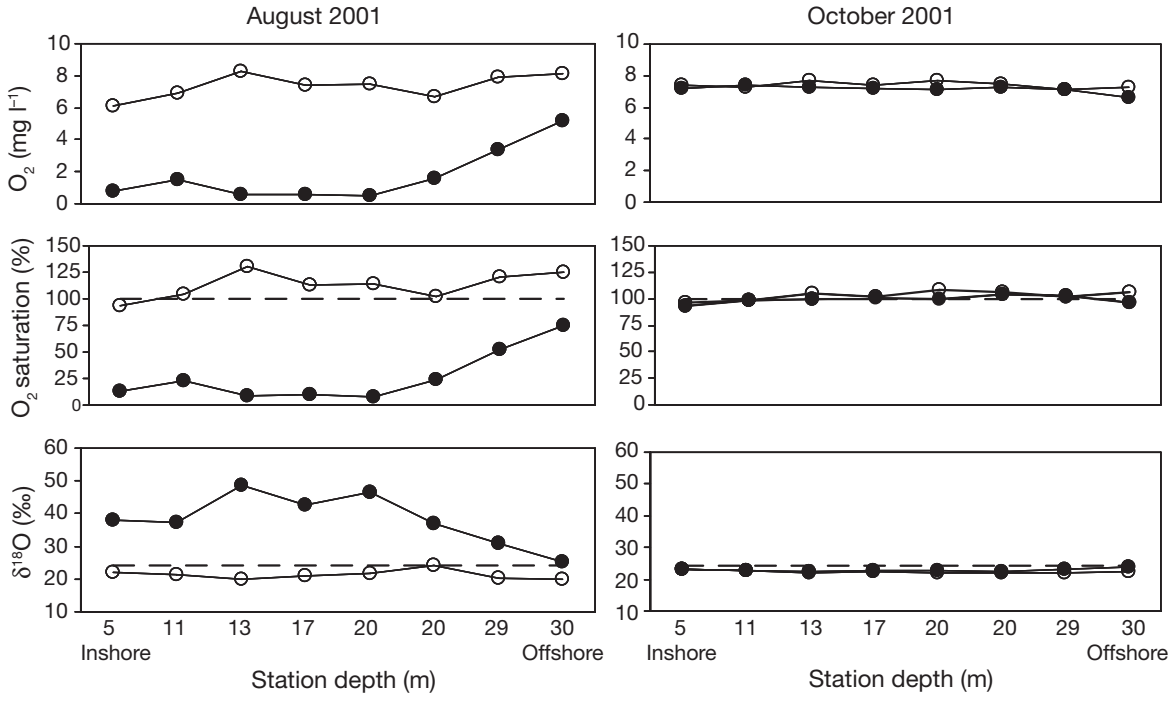

Fig. 6. Oxygen concentration, oxygen saturation and $\delta^{18}O$ for surface (O) and bottom samples (●) for Transect C, August and October 2001. Dashed horizontal lines in the bottom panels represent air-equilibrated values

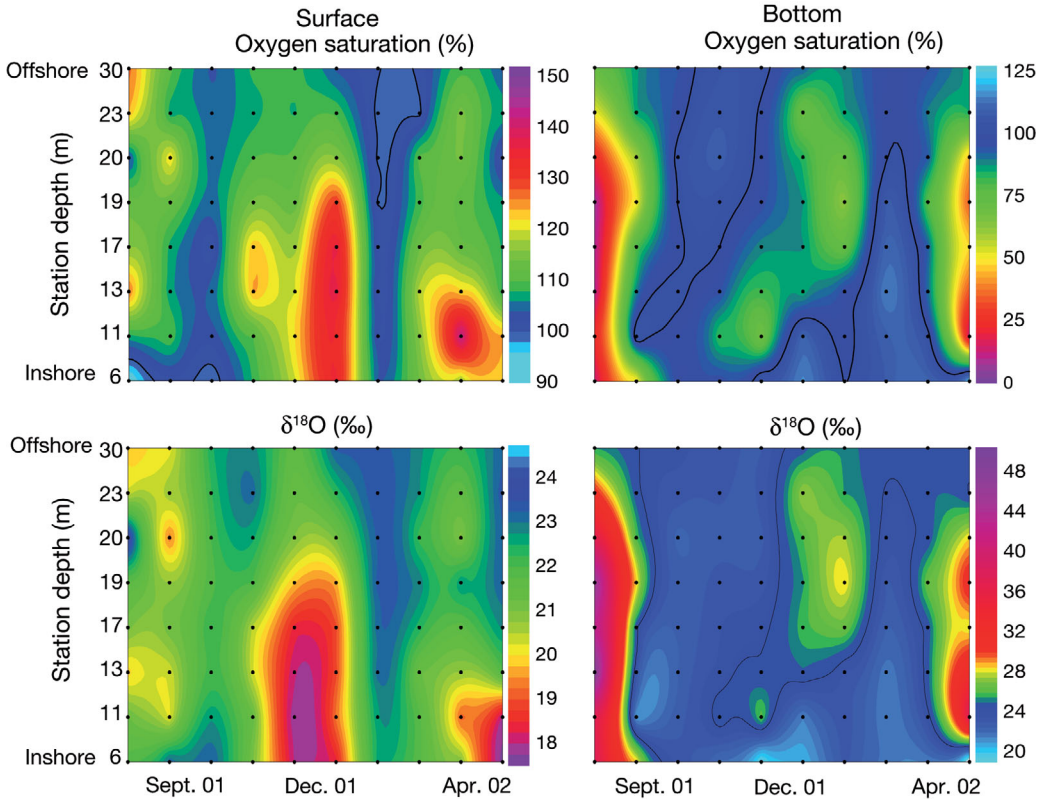

Fig. 7. Oxygen saturation and $\delta^{18}O$ for surface and bottom samples for Transect C, August 2001 to June 2002. The black reference lines represent air-equilibrated values

diurnal pattern was observed across the shelf in surface waters, i.e. high oxygen concentrations (indicated by green shading, top panel Fig. 8) generally occurred during the late afternoon, while lower oxygen concentrations occurred at night and in the early morning, but also in some offshore areas (Fig. 8). Surface $\delta^{18}O$ values were almost always lower than 24.2‰, the value for air-equilibrated water. At the sites of highest O_2 concentrations isotope values were less than 20‰, which is consistent with high rates of primary production. The diurnal pattern observed in oxygen concentrations was even more pronounced for isotope values and lowest $\delta^{18}O$ values were observed in the late afternoon (Fig. 8).

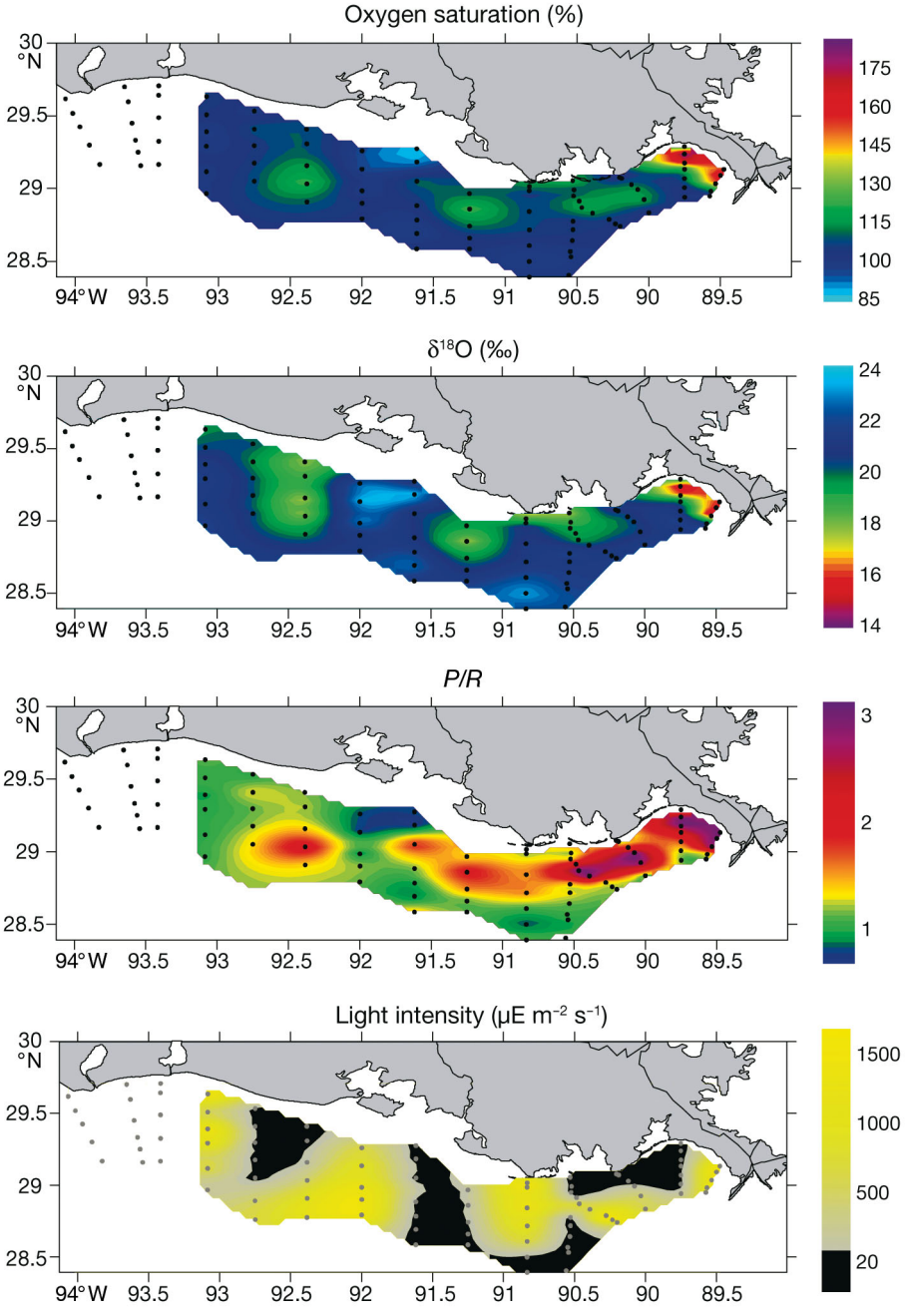

Fig. 8. Oxygen saturation, $\delta^{18}O$, *P/R* and light intensity for surface samples collected during the shelf-wide cruise, July 2001. (●) Sampling grid. *P/R* values that could not be resolved (4 stations near the mouth of the Mississippi River where O_2 saturation exceeded 150%) were set to 3 to facilitate visual perception of the spatial *P/R* pattern

Our *P/R* surface model performed well and captured most of the observed variability in oxygen concentration versus $\delta^{18}O$; of 72 stations sampled we could generate *P/R* values for 68 of them. Only for stations near the mouth of the Mississippi River where oxygen saturation exceeded 150%, could *P/R* not be resolved, even though oxygen supersaturation suggested that *P/R* at these stations was rather high. Calculated *P/R* values of surface samples for the shelf-wide cruise in July 2001 generally exceeded 1 (Fig. 8), which is in agreement with the observed oxygen supersaturation and $\delta^{18}O$ values below 24.2‰. Average (median) *P/R* was 1.12 and the 10th and 90th percentiles were 0.94 and 1.64, respectively. The highest *P/R* values were found near the mouth of the Mississippi River (>2) and in the central part of the Louisiana continental shelf at stations with water depths between 10 and 30 m ($P/R \approx 1.3$). Nevertheless, this pattern was disrupted near the mouth of the Atchafalaya River where we encountered *P/R* values less than 1. Because of the nature of our model (see 'Modeling approach'), *P/R* values did not show the diurnal signal that was observed in oxygen concentrations and $\delta^{18}O$ time series. Rather, our calculated *P/R* values reflect longer term rather than 24 h oxygen cycling as the magnitude of the effects of production (difference between $\delta^{18}O$ of ambient water and dissolved oxygen) and respiration (ε) on $\delta^{18}O$ values were roughly similar at approximately 22‰. Assuming a respiration rate of 0.07 g O_2 m^{-3} h^{-1} and an oxygen to carbon ratio of 3.47 by weight (i.e. Redfield ratio × ratio

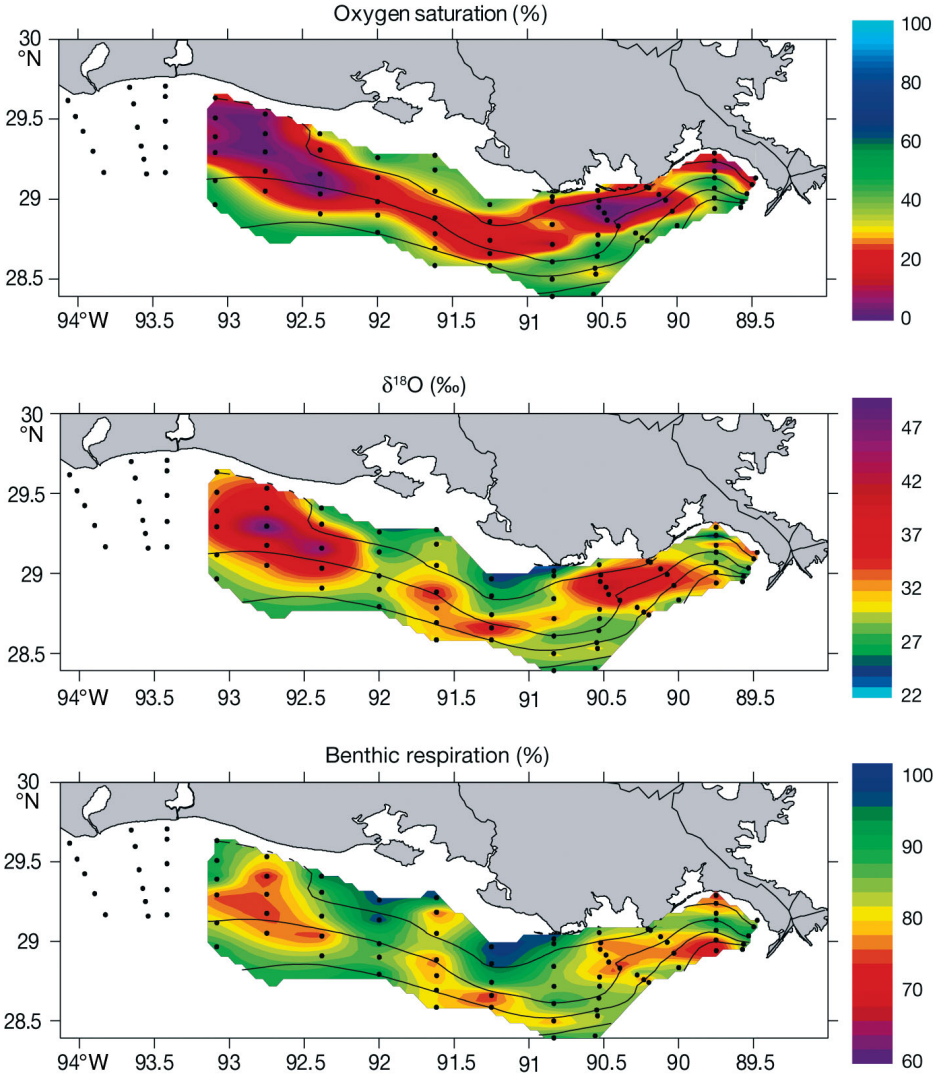

Fig. 9. Oxygen saturation, $\delta^{18}O$ and spatial distribution of benthic respiration for bottom samples collected during the shelf-wide cruise, July 2001. Values for benthic respiration were obtained from a mixing model (see 'Materials and Methods') with 100% water column respiration consistent with a –18‰ respiratory fractionation and 100% benthic respiration consistent with 0‰ fractionation. (●) Sampling grid; lines indicate increasing depth (10, 20, 30, 40 m) as in Fig. 2

of g mol^{-1} O_2/g mol^{-1} C; 1.3 × 2.66 = 3.47), the *P*/*R* values of 0.94, 1.12, and 1.64 (10th percentile, median, 90th percentile) would translate into surface net primary productivities of –0.03, 0.06 and 0.31 g C m^{-3} d^{-1}, respectively, while gross primary production would amount to 0.46, 0.54 and 0.79 g C m^{-3} d^{-1}, respectively.

Bottom water dynamics in July 2001

Bottom water oxygen concentrations were always below 4 mg l^{-1} and hypoxia (dissolved oxygen < 2 mg l^{-1}) was most severe at shallow inshore and mid-stations with water depths up to 30 m (Fig. 9). Hypoxia was especially pronounced in 2 areas located approximately 100 km west of the Mississippi River and 100 km west of the Atchafalaya River. Bottom $\delta^{18}O$ values were usually higher than 24.2‰, particularly in hypoxic waters where $\delta^{18}O$ values could exceed 40‰. The highest $\delta^{18}O$ values were found in the 2 hotspots approximately 100 km west of the Mississippi and Atchafalaya rivers at water depths of 20 to 30 m, coinciding with the lowest oxygen concentrations (Fig. 9).

For respiration in bottom waters the calculated fractionation factor for all samples combined was –6‰ (Fig. 10), which is noticeably less than the –22‰ value that we measured for water column respiration (from incubation experiments). According to our mixing model that separated the effects of benthic versus water column respiration as components of total respiration in bottom waters, we estimated that respiration partitioned 73% to benthic and 27% to water column processes. In addition, water column contributions to total respiration never exceeded 40%. However, the small variation in water column contribution resulted in interesting spatial patterns with the overall somewhat counterintuitive result that water column respiration had larger contributions in areas of very intense hypoxia (Fig. 9). The most intense benthic respiration was found near the mouth of the Atchafalaya River at water depths below 10 m.

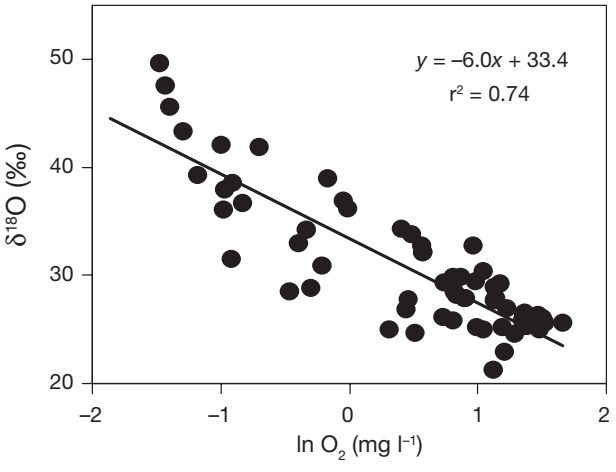

Fig. 10. Relationship between $\delta^{18}O$ and ln (O_2 concentration) for bottom samples collected within 1 m of the sediment during the shelf-wide cruise, July 2001. The slope of the regression line represents the overall average fractionation factor (ε, ‰) due to respiration in bottom water samples

DISCUSSION

We found very large fluctuations in oxygen concentrations and $\delta^{18}O$ values along the productive coastal shelf adjacent to the Mississippi River delta, which indicated that biological processes were very important and dominated oxygen dynamics during summer stratification. In 2001 the Mississippi River discharge was very high and we observed the largest hypoxic area on record, exceeding 20 000 km^2 (Rabalais et al. 2002). The variability of oxygen concentrations versus $\delta^{18}O$ values was not random and enhanced our understanding of oxygen dynamics beyond previous studies that relied on the use of concentration measurements alone.

Surface water dynamics

The combined use of oxygen concentrations and $\delta^{18}O$ values allowed us to estimate *P*/*R* values and, subsequently, net and gross primary productivity across the Louisiana continental shelf. These large scale measurements would not be possible with traditional, more time consuming incubations using either ^{14}C or ^{18}O additions (Grande et al. 1989, Lohrenz et al. 1999). Our estimates of surface net primary productivity ranged from roughly 0 to 0.8 g C m^{-3} d^{-1}, approximately 1 order of magnitude lower than values measured using ^{14}C incubations between 1988 and 1992 across the Louisiana shelf (0 to 10 g C m^{-2} d^{-1}, Lohrenz et al. 1999). The lower values of our study were likely due to the fact that we estimated productivity for the surface layer (approximate depth of 1 m), while Lohrenz et al. (1999) reported depth-integrated primary production for the mixed layer with a depth of generally 5 to 10 m. Assuming no significant light limitation throughout the mixed layer, our values can be transformed from g C m^{-3} d^{-1} to g C m^{-2} d^{-1} by multiplying by a factor of 5 to 10. Then, our productivity estimates would be only slightly lower than those measured by Lohrenz et al. (1999), especially since ^{14}C incubations results usually exceed net primary production (Grande et al. 1989). On the other hand, Justić et al. (1996) calculated average (1985 to 1992) net primary productivities for May

and July of 1.0 and 0.04 C m^{-2} d^{-1}, respectively, using oxygen concentration budgets. The high Mississippi River discharge in 2001, which also occurred later in the year than usual, could probably be the reason that our July 2001 estimates were more representative of productive spring conditions rather than the usually less productive summer conditions.

The spatial pattern of high *P*/*R* and productivity near the mouth of the Mississippi River and along the central part of the shelf was consistent with the Mississippi River as the major nutrient and freshwater source (Rabalais & Turner 2001) and the westerly transport due to the Louisiana–Texas current (Wiseman et al. 1997). The exceptionally low *P*/*R* values at the mouth of the Atchafalaya River might be caused by a combination of shallow water depth, high turbulence, and high turbidity, which would limit productivity despite high nutrient concentrations.

Absolute values of our *P*/*R* and productivity estimates were susceptible to changes in respiration rate and fractionation factor (ε) during respiration. The determined respiration rate of 0.07 mg l^{-1} h^{-1} appears reasonable for the encountered warm and organic-rich bottom waters, as it corresponds to the upper range of values reported by Dortch et al. (1994) for coastal and estuarine system around the world. Typical fractionation factors reported in previous studies encompass our value (–22‰) and range from –15 to –25‰ (Kroopnick 1975, Bender & Grande 1987, Guy et al. 1989, Quay et al. 1993, 1995, Luz et al. 2005). Some of the described variability in net fractionation factors in aquatic systems is probably due to processes that generally occur during light respiration. For example, the importance of Mehler reaction (ε = –15‰), alternative oxidase pathway (ε = –31‰), and photorespiration (ε = –21‰) relative to total respiration will affect the net fractionation factor (Luz et al. 2002). Yet, assuming ε to be –18 or –25‰ (instead of the measured –22‰), *P*/*R* and productivity estimates would only be slightly lower and higher, respectively (Table 1), and the spatial patterns would remain the same. Furthermore, our calculated *P*/*R* values are in agreement with measured *P*/*R* values for a number of coastal ocean systems (ranging from about 0.8 to 4; Williams et al. 1999, Smith & Kemp 2001). Hence, our calculated *P*/*R* and productivity values are generally consistent with productivity patterns in surface shelf waters.

Yet, because of the nature of our model, *P*/*R* values are estimates at this time, with no *P* or *R* measurements made during the 2001 shelf-wide cruise that would directly confirm or refute these values. The modeling approach used to generate these *P*/*R* values was simplistic, assuming that *P* and *R* are always coupled in essentially daytime conditions. Also, an alternative interpretation of *P* and *R* dynamics could not be rejected, namely that *P*/*R* values varied over a smaller range (e.g. 0.9 to 1.4), with larger 'apparent *P*/*R*' variations due to increases in the fractionation factor for respiration, ε_R (–15 from –25‰) rather than changes in *P* or *R*. The total range in ε_R fractionation values from a variety of aquatic and terrestrial environments can extend considerably beyond the central –22‰ fractionation factor assumed for our modeling, from about –4 to –32‰ (Lane & Dole 1956, Kroopnick 1975, Bender & Grande 1987, Guy et al. 1989, Kiddon et al. 1993, Quay et al. 1993, 1995). Still larger *P*/*R* values and larger fractionation factors would both reflect higher productivity in supply–demand isotope models (Fry 2006), and an overall conservative conclusion from the modeling is that the *P*/*R* map of Fig. 8 is likely correct in relative terms of areas of lower and higher productivity, even if there is some uncertainty about the absolute *P*/*R* values. Given these caveats, direct experimental determinations of *P* and *R* during future cruises will be needed to better constrain the *P*/*R* model estimates generated with oxygen concentration and oxygen isotope measurements.

Bottom water dynamics

The combined oxygen concentration and $\delta^{18}O$ measurements of bottom water samples allowed us to differentiate between water column respiration and benthic sediment respiration. For our bottom water samples we observed an overall net fractionation factor of –6‰ (Fig. 10), which is considerably smaller than our measured –22‰ ε_R value for water column respi-

Table 1. Model results of *P*/*R* and gross and net primary production for fractionation factors of –18, –22, and –25‰. Respiration rate was held constant at 0.07 mg O_2 l^{-1} h^{-1} for all 3 scenarios. Values are 10th, 25th, 50th (i.e. median), 75th and 90th percentiles

Fractionation factor (ε_R)	P/R					Gross primary production (g C m^3 d^{-1})					Net primary production (g C m^3 d^{-1})				
	10th	25th	med.	75th	90th	10th	25th	med.	75th	90th	10th	25th	med.	75th	90th
–18‰	0.89	1.11	1.22	1.45	2.17	0.44	0.54	0.60	0.71	1.06	–0.05	0.05	0.11	0.22	0.57
–22‰	0.94	1.06	1.12	1.24	1.64	0.46	0.51	0.54	0.60	0.79	–0.03	0.03	0.06	0.12	0.31
–25‰	0.96	1.03	1.07	1.32	1.32	0.46	0.50	0.52	0.79	0.64	–0.02	0.01	0.03	0.08	0.15

ration. Results of our mixing model indicated that benthic respiration was clearly the dominant sink for dissolved oxygen whereby respiration in the bottom waters was about 75% sediment-driven and 25% water-column-driven. This result is in agreement with previous work by Dortch et al. (1994) who came to a similar conclusion by measuring enzymatic respiratory electron transport system activity (ETS) on the Louisiana continental shelf in July 1991. The dominance of benthic respiration is probably related to the relatively shallow water depth and high sedimentation rates of phytoplankton cells and fecal pellets (Dortch et al. 2001). Consistent with this conclusion we found that benthic respiration was strongest in shallow water (less than 10 m; Fig. 9).

Our calculations of the contribution of benthic respiration to total respiration were based on the assumptions that oxygen inputs to bottom waters from photosynthesis and mixing were both negligible during summertime conditions, i.e. the system was isolated or closed to inputs and exports. These assumptions are supported by the following 3 findings. First, the vertical oxygen transport across the pycnocline in the inner section of the hypoxic zone is small during the peak of summer stratification (Justić et al. 1996). Second, a strong tidal signal, which would indicate horizontal transport, is not present in the periodograms of oxygen data series from station C6B (Rabalais et al. 1994). The maximum lateral displacement of water parcels that can be expected due to diurnal and semidiurnal currents in the study area is only about 3 km (Rabalais et al. 1994), which is not likely to affect the inner section of a 60 km wide hypoxic zone. Third, benthic photosynthesis, which can potentially re-supply significant amounts of oxygen lost by respiration in coastal waters (Dortch et al. 1994, Jahnke et al. 2000), was likely not an important oxygen source for bottom waters in July 2001. At that time light conditions in bottom waters were unfavorable for benthic primary production because Secchi depths were relatively shallow so that little light reached benthic sediments (Fig. 11). Sediments were usually deeper than 2 to 3× Secchi depths, with depths exceeding 2× Secchi depth usually considered to be below the compensation depth for phytoplankton growth (Wetzel 2001). Moderate oxygen inputs due to benthic photosynthesis or oxygen rich surface water would have slightly reduced our estimate of benthic respiration. Nevertheless, even a 20% addition from either source (e.g. conditions reported for July 1991 by Dortch et al. 1994) to the ambient bottom water concentrations would not have had a strong effect on our calculations for the contribution of benthic respiration (Fig. 12). A somewhat smaller or larger fractionation factor for water column respiration, such as –18‰ or –25‰ (Kroopnick 1975, Bender & Grande

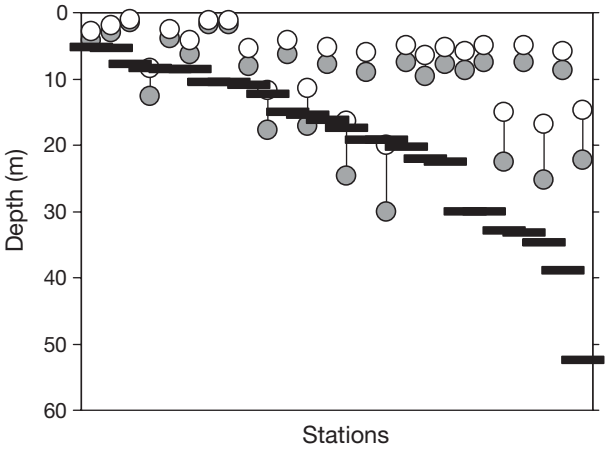

Fig. 11. Relationship between 2× Secchi depth (○) and 3× Secchi depth (●) versus station depth (m, black bars) for the shelf-wide cruise, July 2001

1987, Guy et al. 1989, Quay et al. 1993) would have changed the contribution of benthic respiration as well. Still, in those cases the average contributions of benthic respiration would remain high (66% and 76%, respectively) and the sediment would be the dominant sink for oxygen. On the other hand, a fractionation factor >0‰ for benthic respiration would have underesti-

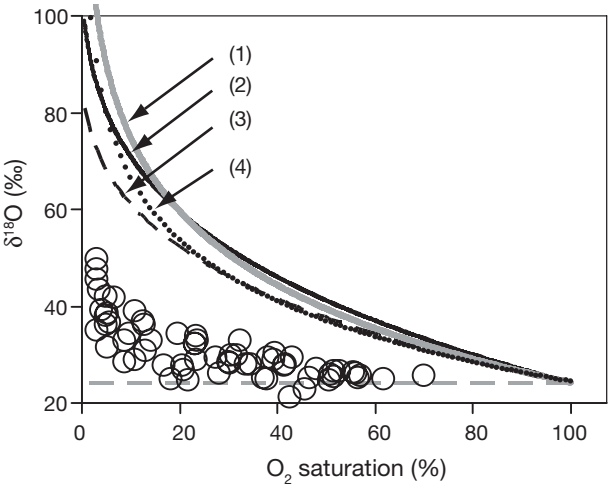

Fig. 12. Relationship between oxygen saturation and $\delta^{18}O$ for bottom water samples (○) collected during the shelf-wide cruise, July 2001. The dashed gray horizontal line represents 100% benthic respiration in the absence of new oxygen inputs, while curved lines represent alternate model scenarios, as follows: (1) grey line: –22‰ fractionation during water column respiration in a closed system with no oxygen inputs; (2) solid black line: as scenario 1, but with a 20% oxygen addition from oxygen rich surface water; (3) black dashed line: as scenario 1, but with a 20% oxygen addition from benthic photosynthesis; (4) dotted line: as scenario 1, but a fractionation factor of –18‰ during water column respiration. The closer a sample is to the lower horizontal line, the larger is the contribution of benthic respiration

mated the contribution of benthic respiration, e.g. an ε value of –3‰ would have increased the average contribution of benthic respiration from 73 to 84%. Brandes & Devol (1997) performed benthic chamber incubations in Puget Sound and measured fractionation factors between –1 to –4‰ for dissolved oxygen. However, the overlaying water in those experiments remained unfiltered and still contained particles that could have contributed to water column respiration, which would explain the measured non-zero fractionation factor.

Our assumed respiration rate of 0.07 mg l^{-1} h^{-1} might have overestimated the actual respiration rate in bottom waters as previous research indicated that respiration rates in surface waters frequently exceed those in bottom waters (Dortch et al. 1994). Nevertheless, beyond the analyses shown in Fig. 12 the conclusions derived from our model that separates water-column and benthic respiration in bottom waters only depended on the fractionation factor of respiration (ε), but were insensitive to the actual respiration rates. A lower respiration rate would lead to the same combinations of oxygen concentration and $\delta^{18}O$ values, but at a later time. In conclusion, our calculated contributions of benthic respiration to total respiration could vary somewhat, but the overall importance of benthic respiration and its spatial patterns remain the same.

The spatial distribution of benthic versus water column respiration indicated that the contribution of water column respiration was larger in areas of intense hypoxia. It is possible that benthic respiration due to the accumulation of organic material on the sediment surface could be relatively similar across the shelf. Areas of high production could contribute further to oxygen loss by water column respiration due to the increased amount of sinking particles. Hence, this combined respiration would then lead to more severe hypoxia along with larger contributions of water column respiration. This assumption is also supported by increased *P*/*R* in the central part of the Louisiana shelf, which should result in increased particle flux to the lower water column. Similar to the low *P*/*R* values, the highest contribution of benthic respiration in the vicinity of the Atchafalaya River delta might be a result of high turbidity in these areas (due to high concentrations of suspended phytoplankton and sediment) in combination with a relatively shallow water column of generally less than 10 m. The lack of particle flux due to low *in situ* production and a reduced depth as potential site for water column respiration would favor the dominance of benthic respiration at the shallower stations. Reduced oxygen concentrations in areas of strong hypoxia may also impose a diffusional limitation on sediment respiration rates, increasing the apparent importance of water column respiration.

Acknowledgements. This work was funded by the National Oceanographic and Atmospheric Administration Coastal Ocean Program grant for hypoxic studies (NA06OP0526). We are particularly grateful to N. N. Rabalais for organizing and leading the shelf-wide and monthly cruises, also funded by NOAA Coastal Ocean Program (NA06OP0528). Z.J.Q.-R. was supported by a grant from the J. Bennett Johnston Science Foundation. N. N. Rabalais provided surface PAR, oxygen, salinity and temperature data that were incorporated in this work. R. E. Turner provided Secchi depth readings. The crews of the R/V 'Pelican' and R/V 'Acadiana' provided important technical field support. Finally, we thank N. Atilla, A. Barker, B. Cole, V. Gudatti, J. Lee, and C. Milan, for their assistance in the field and laboratory, as well as N. N. Rabalais, N. Ostrom and 3 anonymous reviewers for their helpful comments on an earlier version of this manuscript.

LITERATURE CITED

Barkan E, Luz B (2005) High precision measurements of $^{17}O/^{16}O$ and $^{18}O/^{16}O$ ratios in H_2O. Rapid Commun Mass Spectrom 19:3737–3742

Bender ML, Grande K (1987) Production, respiration and the isotopic geochemistry O_2 in the upper water column. Global Biogeochem Cycles 1:49–59

Benson BB, Parker DM (1961) Nitrogen/argon isotope ratios in aerobic sea water. Deep-Sea Res 7:237–264

Brandes JA, Devol AH (1997) Isotopic fractionation of oxygen and nitrogen in coastal marine sediments. Geochim Cosmochim Acta 61:1793–1802

Craig H, Hayward T (1987) Oxygen supersaturation in the ocean: biological versus physical contributions. Science 235:199–202

Diaz RJ, Rosenberg R (1995) Marine benthic hypoxia: a review of its ecological effects and behavioural responses of benthic macrofauna. Oceanogr Mar Biol Annu Rev 33: 245–303

Dinnel S, Wiseman WJ Jr (1986) Freshwater on the Louisiana shelf. Cont Shelf Res 6:765–784

Dole M, Lane GA, Rudd DP, Zaukelies DA (1954) Isotopic composition of atmospheric oxygen and nitrogen. Geochim Cosmochim 6:65–78

Dortch Q, Turner RE, Rowe GT (1994) Respiration rates and hypoxia on the Louisiana shelf. Estuaries 17:862–872

Dortch Q, Rabalais NN, Turner RE, Qureshi NA (2001) Impacts of changing Si/N ratios and phytoplankton species composition. In: Rabalais NN, Turner RE (eds) Coastal hypoxia: consequences for living resources and ecosystems. Coast Estuar Stud 58, American Geophysical Union, Washington, DC, p 37–48

Emerson S, Stump C, Wilbur D, Quay P (1999) Accurate measurement of O_2, N_2, and Ar gases in water and the solubility of N_2. Mar Chem 64:337–347

Fry B (2006) Stable isotope ecology. Springer, New York

Grande KD, Williams PJ, Marra J, Purdie DA, Heinemann K, Eppley RW, Bender ML (1989) Primary production in the North Pacific gyre: a comparison of rates determined by the ^{14}C, O_2 concentration and ^{18}O methods. Deep-Sea Res 36:1621–1634

Guy RD, Berry JA, Fogel ML, Hoering TC (1989) Differential fractionation of oxygen isotopes by cyanide-resistant and cyanide-sensitive respiration in plants. Planta 177: 483–491

Guy RD, Fogel ML, Berry JA (1993) Photosynthetic fractionation of the stable isotopes of oxygen and carbon. Plant Physiol 101:47–47

Hickel W, Mangelsdorf P, Berg J (1993) The human impact in the German Bight: eutrophication during three decades (1962–1991). Helgol Wiss Meeresunters 47:243–263

Jahnke RA, Nelson JR, Marinelli RL, Eckman JE (2000) Benthic flux of biogenic elements on the southeastern US continental shelf: influence of pore water advective transport and benthic microalgae. Cont Shelf Res 20:109–127

Justić D, Legović T, Rottini-Sandrini L (1987) Trends in the oxygen content 1911–1984 and occurrence of benthic mortality in the northern Adriatic Sea. Estuar Coast Shelf Sci 25:435–445

Justić D, Rabalais NN, Turner RE (1996) Effects of climate change on hypoxia in coastal waters: a doubled CO_2 scenario for the northern Gulf of Mexico. Limnol Oceanogr 41:992–1003

Kampbell DH, Wilson JT, Vandergrift SA (1989) Dissolve oxygen and methane in water by a GC headspace equilibration technique. Int J Environ Anal Chem 36:249–257

Kiddon, J, Bender ML, Orchardo J, Caron DA, Goldman JC, Dennett M (1993) Isotopic fractionation by respiring marine organisms. Global Biogeochem Cycles 7:679–694

Knox M, Quay PD, Wilbur D (1992) Kinetic isotope fractionation during air–water gas transfer of O_2, N_2, CH_4, and H_2. J Geophys Res 97:20335–20343

Kroopnick PM (1975) Respiration, photosynthesis, and oxygen isotope fractionation in oceanic surface water. Limnol Oceanogr 20:988–992

Lane GA, Dole M (1956) Fractionation of oxygen isotopes during respiration. Science 123:574–576

Lohrenz SE, Dagg MJ, Whitledge TE (1990) Enhanced primary production in the plume/oceanic interface of the Mississippi River. Cont Shelf Res 10:639–664

Lohrenz SE, Fahnenstiel GL, Redalje DG, Lang GA, Dagg MJ, Whitledge TE, Dortch Q (1999) Nutrients, irradiance, and mixing as factors regulating primary production in coastal waters impacted by the Mississippi River plume. Cont Shelf Res 19:1113–1141

Luz B, Barkan E, Sagi Y, Yacobi Y (2002) Evaluation of community respiratory mechanisms with oxygen isotopes: a case study in Lake Kinneret. Limnol Oceanogr 47:33–42

Mariotti A, Germon JC, Hubert P, Kaiser P, Letolle R, Tardieux A, Tardieux P (1981) Experimental determination of nitrogen kinetic isotope fractionation: some principles; illustration for the denitrification and nitrification processes. Plant Soil 62:413–430

Miyajima T, Yamada T, Hanba YT (1995) Determining the stable isotope ratio of total dissolved inorganic carbon in lake water by GC/C/IRMS. Limnol Oceanogr 40:994–1000

Officer CC, Biggs RB, Taft JL, Cronin LE, Tyler M, Boynton WR (1984) Chesapeake Bay anoxia: origin, development and significance. Science 223:22–27

Ostrom NE, Carrick HJ, Twiss MR (2005) Evaluation of primary production in Lake Erie by multiple proxies. Oecologia 145:669–669

Pavella JS, Ross JL, Chittenden ME Jr (1983) Sharp reduction in abundance of fishes and benthic macroinvertebrates in the Gulf of Mexico off Texas associated with hypoxia. Northeast Gulf Sci 6:167–173

Quay PD, Emerson S, Wilbur DO, Stump C (1993) The ‰^{18}O of dissolved O_2 in the surface waters of the Subarctic Pacific: a tracer of biological productivity. J Geophys Res 98:8447–8458

Quay PD, Wilbur DO, Richey JE, Devol AH, Benner R, Forsberg BR (1995) The ^{18}O:^{16}O of dissolved oxygen in rivers and lakes in the Amazon basin: Determining the ratio of respiration to photosynthesis rates in freshwaters. Limnol Oceanogr 40:718–729

Rabalais NN, Wiseman WJ Jr, Turner RE (1994) Comparison of continuous records of near-bottom dissolved oxygen from the hypoxic zone along the Louisiana coast. Estuaries 17:850–861

Rabalais NN, Turner RE (eds) (2001) Coastal hypoxia: consequences for living resources and ecosystems. Coast Estuar Stud 58, American Geophysical Union, Washington, DC

Rabalais NN, Turner RE, Scavia D (2002) Beyond science into policy: Gulf of Mexico hypoxia and the Mississippi River. BioScience 52:129–142

Sklar FH, Turner RE (1981) Characteristics of phytoplankton production off Barataria Bay in an area influenced by the Mississippi River. Contrib Mar Sci 24:93–106

Smith EM, Kemp WM (2001) Size structure and production/respiration balance in a coastal plankton community. Limnol Oceanogr 46:473–485

Stigebrandt A (1991) Computations of oxygen fluxes through the sea-surface and the net production of organic matter with application to the Baltic and adjacent seas. Limnol Oceanogr 36:444–454

Turner RE, Rabalais NN (1994) Evidence for coastal eutrophication near the Mississippi River delta. Nature 368: 619–621

Turner RE, Rabalais NN, Justić D, Dortch Q (2003) Global patterns of dissolved N, P and Si in large rivers. Biogeochemistry 64:297–317

Weiss R (1970) The solubility of nitrogen, oxygen and argon in water and seawater. Deep-Sea Res 17:721–735

Wetzel RG (2001) Limnology, lake and river ecosystems, 3rd edn. Academic Press, San Diego, CA

Williams PJB, Bowers DG, Duarte CM, Agosti S, delGiorgio PA, Cole JJ (1999) Regional carbon imbalances in the oceans. Science 284:1735b

Wiseman WJ Jr, Rabalais NN, Turner RE, Dinnel SP, MacNaughton A (1997) Seasonal and interannual variability within the Louisiana coastal current: stratification and hypoxia. J Mar Syst 12:237–248

Editorial responsibility: Lisa Levin (Contributing Editor), La Jolla, California, USA

Submitted: June 2, 2006; Accepted: December 10, 2006
Proofs received from author(s): July 5, 2007